

Optimization of grid-connected microgrid consisting of PV/FC/UC with considered frequency control

Hamid HASSANZADEHFARD, Seyed Masoud MOGHADDAS-TAFRESHI, Seyed Mehdi HAKIMI*
Faculty of Electrical Engineering, K.N. Toosi University of Technology, Tehran, Iran

Received: 13.11.2011 • Accepted: 29.04.2012 • Published Online: 12.01.2015 • Printed: 09.02.2015

Abstract: In this paper, ultracapacitors are used as short-term storages for the frequency control of grid-connected microgrid that consists of photovoltaic panels, fuel cells, and the battery packs as long-term storages. Fuel cells and battery packs have delays in load tracking; therefore, ultracapacitors are used to compensate for the sudden power fluctuations in the microgrid that occur due to the output power uncertainty of the PV arrays and the loads required in the microgrid, as well as the sudden interruption of the main grid. The microgrid consists of interruptible and uninterruptible loads. When the total produced power in the microgrid, in addition to the purchased power from the grid, cannot satisfy the demand, first, the interruptible loads, and then the uninterruptible loads, are interrupted. In this paper, the forced outage rate of each component and some notions of the reliability are considered for the microgrid. To ensure the system's reliability, the uncertainty of the PV power and load demand is considered.

Key words: Forced outage rate, frequency control, reliability, ultracapacitor, uncertainty

1. Introduction

Due to the growing demand for renewable energy sources, the manufacturing of solar cells and photovoltaic (PV) arrays and wind turbines has advanced considerably in recent years. Hence, the cost of PVs and wind turbines has declined steadily since the first solar cells and wind turbines were manufactured. They can replace some of the fossil energy sources to reduce the greenhouse gas emissions and air pollution. The increase in the penetration of distributed generation and the presence of multiple distributed generators in electrical proximity to one another have brought about the concept of the microgrid [1,2].

The concept of the microgrid was first proposed by the Consortium for Electric Reliability Technology Solutions (CERTS) in America; it is a new type of distributed generation network structure with a wide range of development prospects [3]. Microgrids comprise low-voltage distribution systems with distributed energy sources, storage devices, and controllable loads that are operated either islanded or connected to the main power grid in a controlled, coordinated way. The authors in [4,5] introduced the benefits of the microgrid, such as enhanced local reliability, reduced feeder losses, and local voltage support, providing increased efficiency using waste heat as combined heat and power, voltage sag correction, or providing uninterruptible power supply functions. The steady progress in the development of distributed power generation, such as microgrids and renewable energy technologies, are opening up new opportunities for the utilization of energy resources.

The power generated by a PV system and wind turbine [6] is highly dependent on the weather conditions. For example, during cloudy periods and at night, a PV system would not generate any power [7]. Battery packs

*Correspondence: sm_hakimi@iee.org

are used as a long-term energy storage system to use solar and wind energy resources more efficiently and economically [8]. Ultracapacitors (UCs) as short-term energy storage are used to compensate for transient conditions because they can be charged and recharged rapidly in the condition of uncertainty and sudden interruption.

Maintaining the frequency at its target value requires that the produced and consumed active power is controlled to keep the load and generation in balance. A certain amount of active power, usually called the frequency control reserve, is kept available to perform this control [9].

For standalone hybrid wind/PV power systems, a typical tangent method is used to fix the size of the wind generator and optimize the size of the PV panels and the capacity of the batteries [10,11]. Several research works have been done for selecting the parameters, such as the size of the wind generators, the size of the PV panels, and the capacity of the batteries, but the decision variables were collectively taken without any optimizing methodologies [10–17].

In [18], a small-scale experiment wind energy kit was prepared in order to introduce renewable energy applications. In [19], the energy demand of a house in Gebze, Turkey, was met using wind energy as a primary energy source combined with rechargeable batteries. The wind turbine generators considered were of various nominal powers, ranging from 0.6 to 450 kW. For each wind turbine, the necessary number of batteries to continuously supply the house with energy was calculated and an economic analysis of each system was performed.

An evolutionary algorithm-based optimization for designing a standalone multisource hybrid power system was presented in [20], such as a wind farm, PV array, diesel generator, and battery pack. In this work, the battery pack has been used to cover the emergency loads energy.

The authors in [21] presented an optimized design of a grid-connected multisource hybrid power system, including sources like a PV array, electrolyzer, fuel cell (FC), H₂-tank, and grid electricity based on the genetic algorithm (GA). In this work, grid electricity was used to cover the demand loads when renewable sources could not produce enough energy. The development of a computational model for the optimal sizing of a solar-wind hybrid energy system was presented in [22]. The authors of [23] presented an automatic procedure to perform the optimal sizing of a grid-connected hybrid solar wind power system developed by a fuzzy logic-based multiobjective optimization approach. In [7], the modeling, control, and simulation of a PV/FC/UC-based hybrid power generation system for standalone applications were studied. The study in [24] focuses on the dynamic behavior of an autonomous wind turbine/PV/FC/UC hybrid power system under various wind speed, solar radiation, and load demand conditions. However, [7] and [24] do not consider the optimal size of the UCs for the frequency control of the microgrid.

Recently, a GA for the concerned problem was proposed by Xu et al. [25], where the GA optimizes the size of the wind generators, the size of the PV panels, and the capacity of the batteries as decision variables. Although this method provides a better performance in comparison to the previous literature sources, it is necessary to find a flexible generalized methodology for any kind of microgrid designed with a higher computational efficiency. In [26], a GA is used to improve the maximum power point tracking efficiency of a PV system with an induction motor drive by optimizing the input dataset for an artificial neural network model of the PV modules.

Long-term energy storage is needed in this system due to the intermittent nature of solar energy and short-term energy storage is needed to compensate for the uncertainty and sudden interruption. The system uses the natural gas to produce its required hydrogen. The generation of hydrogen by the reformer causes a higher reliability for the system.

This study was performed for the Ganje site in northwestern Iran. It is located in a village with a population of 800. This village can exchange power with the grid. Since the demand of this area was previously met by diesel generators, our aim is to minimize the total costs of the system, such that the demand is met and the microgrid responds quickly for sudden changes of demand or produced power due to uncertainty or interruption from the grid.

First, the microgrid is considered and the cost of the system is presented by an objective function. Next, the particle swarm optimization (PSO) algorithm is reviewed. Finally, some simulation results are presented.

Section 2 expresses the microgrid's component descriptions; Section 3 describes the system modeling and strategy and some notions of reliability, forced outage rate (FOR), calculations of uncertainty, and the frequency control of the microgrid, and, finally, the PSO algorithm is reviewed. Section 4 presents the simulation results, and, finally, the conclusion of this study is given.

2. Microgrid components

2.1. PV

The output power of the PV generator P_{PV} can be calculated according to the following equation:

$$P_{PV} = \eta_g * N * A_m * G_t, \quad (1)$$

where η_g is the instantaneous PV generator efficiency that is considered to be 50% in this paper, A_m is the area of a single module used in a system (m^2), G_t is the global irradiance incident on the titled plane (W/m^2), and N is the number of modules. In this analysis, each PV generator has a rated power of 1 kW. The cost of 1 unit considered is US\$4000 while the replacement and maintenance costs are taken as \$3000 and \$0/year, respectively. The lifetime of a PV generator is taken to be 20 years [27].

2.2. Fuel cell

The proton exchange membrane FC is an environmentally clean power generator that combines hydrogen fuel with oxygen from the air to produce electricity. The capital cost, replacement, and operational costs are taken as \$3500 [28], \$3000, and \$175/year for a 1 kW system, respectively. The FC's lifetime is considered to be 5 years. In this study, the efficiency of the FC is considered to be 50%.

2.3. Battery storage

At any hour, the state of the battery is related to the previous state of the charge and to the energy production and consumption situation of the system during the time from $t - 1$ to t .

In all of the cases, the storage battery capacity is subject to the following constraints:

$$E_{bat \min} \leq E_{bat}(t) \leq E_{bat \max}, \quad (2)$$

where $E_{bat \max}$ and $E_{bat \min}$ are the maximum and minimum allowable storage capacities.

$E_{bat \min}$ is determined by the maximum allowable depth of the battery discharge, as follows:

$$E_{bat \min} = (1 - DOD) * E_{bat \max}. \quad (3)$$

In this analysis, each battery pack's capacity is 2.76 kWh. The cost of each battery considered is \$264, while the replacement and maintenance costs are taken as \$260 and \$2.64/year [27]. The lifetime of a battery is taken to be 3 years [27]. The type of battery chosen for this study is the Surrette S460.

2.4. Ultracapacitor

For several years, UCs have received attention as a new energy storage element. UCs have some advantages over batteries [29]:

- High power density.
- Low lifetime, with degradation starting after 100,000 cycles.
- No maintenance, high reliability.
- Environmental safety.
- Wider operating temperature range.

UCs have an extremely fast discharge and charging response, and so in this study, UCs are used for the frequency control of the microgrid.

The storage UC's capacity is subject to the following constraints:

$$E_{uc\min} \leq E_{uc}(t) \leq E_{uc\max}, \quad (4)$$

where $E_{uc\max}$ and $E_{uc\min}$ are the maximum and minimum allowable storage capacities of UC. $E_{uc\min}$ is determined according to the following equation:

$$E_{uc\min} = SOC_{uc} * E_{uc\max}, \quad (5)$$

where $SOC_{uc} = 0.25$ is the minimum allowable state-of-charge level of the UC.

UCs have high reliability, require no periodic maintenance, and have an expected life of 10 years.

In this analysis, the capacity of each UC is considered as 1 Wh. The cost of each UC is considered as \$40, while the replacement cost is taken as \$30 [30].

UCs has high efficiency, and in this paper, it is considered to be 95%.

2.5. Grid connection

Microgrids can exchange power with grids. The surplus produced power of the PV arrays after charging batteries is sold to the grid. If the total produced power of the microgrid cannot satisfy the demand, power will be purchased from the grid.

2.6. Loads

The loads may be interruptible or uninterruptible. The cost of electricity interruptions has been estimated. We assume that in each hour, 10% of loads are interruptible and 90% of loads are uninterruptible, and at any hour, the microgrid can interrupt only 10% of the uninterruptible loads subject to reliability constraints such as the equivalent loss factor (ELF).

3. System modeling and strategy

The microgrid consists of some PV arrays, FCs, reformers, battery packs, and interruptible and uninterruptible loads (Figure 1).

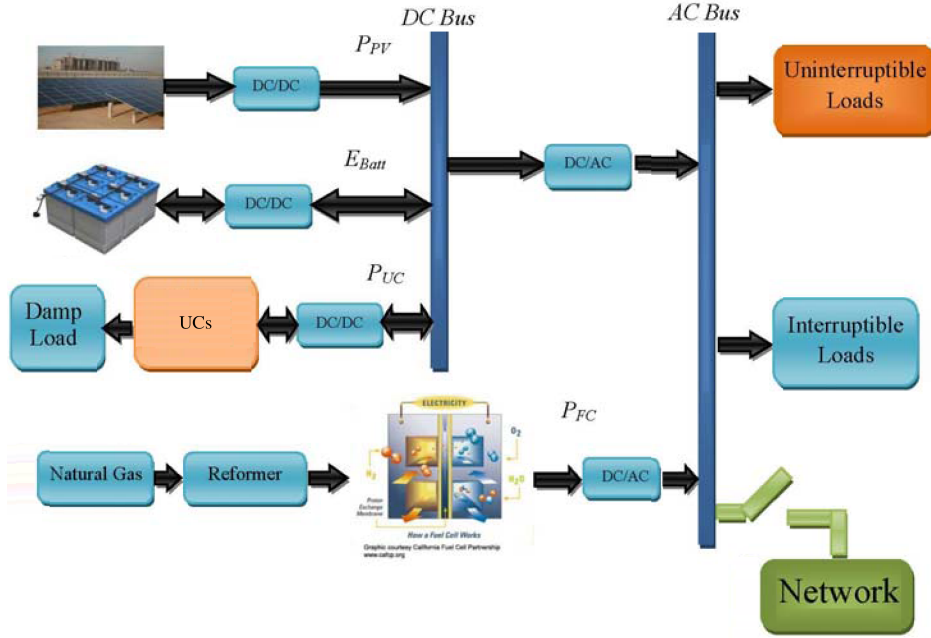


Figure 1. Schematic diagram of microgrid.

It is desirable that the system meets the demand, the costs are minimized, and the components have optimal sizes.

We consider 3 situations for the system: A) the generation power produced by renewable energy (PV arrays) meets the demand, B) over generation, and C) over demand.

A. Generation power produced by the PV arrays meets the demand

In this situation, the power generated by the PV arrays is equal to the demand; hence:

$$P_{PV}(t) = (P_{Load}(t)/\eta_{DC/AC}), \quad (6)$$

$$E_{bat}(t + \Delta t) = E_{bat}(t),$$

$$P_{FC}(t) = 0,$$

$$P_{sell}(t) = 0,$$

$$P_{buy}(t) = 0,$$

where $\eta_{DC/AC}$ is the DC/AC efficiency. It is notable that the time steps Δt are taken to be 1 h in this study.

B. Over generation

The produced power of the PV arrays is more than the demand:

$$P_{PV}(t) > (P_{Load}(t)/\eta_{DC/AC}). \quad (7)$$

The excess power is utilized for charging the batteries:

$$E_{bat}(t + \Delta t) = E_{bat}(t) + (P_{PV}(t) - P_{Load}(t)/\eta_{DC/AC}) * \Delta t * \eta_{cha},$$

$$P_{FC}(t) = 0. \quad (8)$$

$$\eta_{cha}$$

is the battery charger efficiency, and in this paper, it is considered to be 85%. If the surplus produced power of the PV arrays after charging the batteries overflows, this power P_{sell} can be sold to the grid:

$$P_{sell}(t) = \frac{(E_{bat}(t + \Delta t) - E_{bat \max}) * \eta_{DC/AC}}{\Delta t * \eta_{dech}},$$

$$E_{bat}(t) = E_{bat \max}. \quad (9)$$

C. Over demand

The demand is more than the power generated by the PV arrays:

$$P_{PV}(t) < (P_{Load}(t)/\eta_{DC/AC}). \quad (10)$$

In this situation, there are 2 cases:

- 1) The available battery packs' energy and the power generation of the PV arrays can meet the demand:

$$P_{PV}(t) + (E_{bat}(t) - E_{bat \min}) * \eta_{dech}/\Delta t > (P_{Load}(t)/\eta_{DC/AC}). \quad (11)$$

Therefore:

$$E_{bat}(t + \Delta t) = E_{bat}(t) + (P_{PV}(t) - P_{Load}(t)/\eta_{DC/AC}) * \Delta t/\eta_{dech},$$

$$P_{FC}(t) = 0. \quad (12)$$

η_{dech} is the battery discharging efficiency and in this paper, it is considered to be 85%.

- 2) The available battery packs' energy and the power generation of the PV array cannot meet the demand.

In this situation, the battery packs are completely discharged and the energy in the battery packs is equal to $E_{bat \min}$. In this state, load requirements are supplied from the FC P_{FC} :

$$E_{bat}(t + \Delta t) = E_{bat \min},$$

$$P_{FC}(t) = (P_{Load}(t)/\eta_{DC/AC}) - P_{PV}(t) - (E_{bat}(t) - E_{bat \min}) * \eta_{dech}/\Delta t. \quad (13)$$

In this situation, if the total produced power (PV + FC + battery) cannot satisfy the demand, the required power P_{buy} will be purchased from the grid.

$$P_{sell}(t) = 0$$

$$P_{buy}(t) = (P_{FC}(t) - N_{FC} * P_{fuel-cell}) * \eta_{DC/AC} \quad (14)$$

Here, N_{FC} is the optimum size of the FC and $P_{fuel-cell}$ is the rated power of the FC.

3.1. System cost

In this paper, we consider the capital and replacement costs and the operation and maintenance costs of each component of the microgrid. We choose net present cost (NPC) for calculation of the system's cost.

The NPC of each component is defined as [31]:

$$NPC = N * (capital_cost + replacement_cost * K + operation\&maintenance_cost * \frac{1}{CRF(ir, R)}), \quad (15)$$

$$CRF(ir, R) = \frac{ir * (1 + ir)^R}{(1 + ir)^R - 1}, \quad (16)$$

$$K = \sum_{n=1}^y \frac{1}{(1 + ir)^{L*n}}, \quad (17)$$

where L is the lifetime and N is the optimal number of each component.

3.1.1. The objective function

The objective function is the sum of all of the NPCs [32]:

$$NPC = NPC_{PV} + NPC_{battery} + NPC_{FC} + NPC_{UC} + NPC_{reformer} + NPC_{Transe} + NPC_{conv} - NPC_{sell} + NPC_{buy} + NPC_{Pi} + NPC_{Pui}, \quad (18)$$

where NPC_{Pi} and NPC_{Pui} are the NPCs for the interruptible and uninterruptible loads, respectively. NPC_{buy} and NPC_{sell} are the NPCs for the purchased energy from the grid and the sold energy to the grid. NPC_{Pi} , NPC_{Pui} , NPC_{buy} , and NPC_{sell} are described by the following equations:

$$NPC_{buy} = \sum_{t=1}^{8760} P_{buy}(t) * C_{buy} * (1/CRF), \quad (19)$$

$$NPC_{sell} = \sum_{t=1}^{8760} P_{sell}(t) * C_{sell} * (1/CRF), \quad (20)$$

$$NPC_{Pi} = \sum_{t=1}^{8760} Q_i(t) * C_{Penalty-Pi} * (1/CRF), \quad (21)$$

$$NPC_{Pui} = \sum_{t=1}^{8760} Q_{ui}(t) * C_{Penalty-Pui} * (1/CRF), \quad (22)$$

where C_{buy} , C_{sell} , $C_{Penalty-Pi}$, and $C_{Penalty-Pui}$ are the cost of the purchased energy from the grid (\$/kWh), the energy sold to the grid (\$/kWh), and the costs of the electricity interruptions for the interruptible and uninterruptible loads (\$/kWh), respectively.

NPC_{FC} contains both the NPC for the purchased gas from the grid and the NPC for the FC.

$$NPC_{FC} = NPC_{fuel-cell} + NPC_{fuel} \quad (23)$$

The NPC for the purchased gas from the grid NPC_{fuel} is described by the following equation:

$$NPC_{fuel} = \sum_{t=1}^{8760} P_{fc}(t) * C_{fuel} * E / CRF(ir, R). \quad (24)$$

C_{fuel} is the cost of the produced gas ($\$/m^3$) and E is the amount of fuel that is needed to produce 1 kWh of energy by the FC.

Ninety-five percent of natural gas is composed of methane. Each cubic meter of methane is equal to 1.29 m³ of hydrogen gas. The equivalent heating value of hydrogen is 3.4 kWh/m³ at standard conditions. Considering a 50% efficiency for the FC, each cubic meter of hydrogen gas produces 2.083 kWh according to the following equation:

$$1.29(m^3) * 3.4 \frac{kWh}{m^3} * 0.95 * \eta_{fc} = 2.083(kWh). \quad (25)$$

Therefore, the amount of fuel that is needed to produce 1 kWh of energy by the FC is obtained by:

$$E\left(\frac{m^3}{kWh}\right) = \frac{1}{2.083} = 0.48. \quad (26)$$

The objective function must be minimized, which is accomplished by the PSO algorithm in this paper.

3.2. Reliability

Some notions of reliability are commonly used for systems with an hourly demand and supply data. The loss of load expectation (LOLE), loss of energy expectation (LOEE), loss of power supply probability (LPSP), and ELF are some of those considered in this paper.

The ELF is described by:

$$ELF = \frac{1}{N} \sum_{t=1}^N \frac{Q_{ui}(t)}{P_{ui}(t)}, \quad (27)$$

where $P_{ui}(t)$ is the uninterruptible load, $Q_{ui}(t)$ is the loss-of-uninterruptible load, and N is the number of hours.

The ELF contains information about both the number of outages and their magnitude. In this paper, we consider that the ELF should be lower than 0.01 [33].

Other notions of reliability are described in [34,35].

3.3. Forced outage rate

The basic generating unit parameter used in static capacity evaluation is the probability of finding the unit on the forced outage at some distant time in the future. This probability was defined in engineering systems as the unit unavailability, and historically, in power system applications, it is known as the unit FOR.

The FORs of the generating units are known to be a function of unit size and type and, therefore, a fixed percentage reserve cannot ensure a consistent risk.

In this section, the FOR is considered for some of the components in the microgrid. The amounts of the FOR for the PV arrays (FOR_{PV}) and the converters (FOR_{conv}) are equal to 4% and 0.11%, respectively [36].

Therefore, the output power of the PV arrays considering the FOR can be calculated according to the following equation:

$$P_{PV_FOR}(t) = P_{PV}(t) * (1 - FOR_{PV}). \quad (28)$$

For considering the FOR for converters, the efficiency of the converters is multiplied by the availability of converters A_{conv} obtained by the following equation:

$$A_{conv} = (1 - FOR_{conv}). \quad (29)$$

3.4. Calculations of uncertainty

Since there is uncertainty in solar radiation and demand, although this profile is forecasted, there are deviations from the forecasted values. The deviations for the PV power and loads are simulated close to an actual change wave by the following functions, as presented in [37]:

$$dP_{PV} = 0.7 * \sqrt{P_{PV}}, \quad (30)$$

$$dP_{Load} = 0.6 * \sqrt{P_{load}}. \quad (31)$$

Therefore, in this paper, the uncertainty of the PV power and demand are obtained by multiplying the random output fluctuation derived from the white noise block in MATLAB/Simulink.

Therefore, the output power of the PV arrays and demand considering the uncertainty are obtained by the following equations:

$$P_{PV_un} = dP_{PV} * noise + P_{PV}, \quad (32)$$

$$P_{Load_un} = dP_{Load} * noise + P_{Load}. \quad (33)$$

Finally, the output power of the PV arrays considering the FOR and uncertainty are obtained as:

$$P_{PV_un_FOR}(t) = P_{PV_un}(t) * (1 - FOR_{PV}). \quad (34)$$

3.5. Frequency control of the microgrid

The uncertainty of solar radiation and the forecasting load as well as a sudden interruption from the grid causes a frequency deviation in the microgrid. UC banks can be used for short-term energy storage for charging/discharging and, additionally, to meet the instantaneous variations of the produced power or demanded power that occur due to the uncertainty or sudden interruption of the grid.

As another feature, when the microgrid operates in islanded mode, the load tracking delays and mismatches of the FCs and battery packs (3 s) should be compensated for by the UC banks.

Hence, the UCs inject energy into the microgrid during power variations for about 3 s to prevent frequency fluctuations. After these times, the FCs or battery packs inject power into the microgrid.

If grid problems occur when the microgrid works in grid-connected mode, the UCs can provide compensation repeatedly and the microgrid can continue to operate in islanded operation without any interruption in the load requirements.

The minimum size of the UCs for load tracking delays $E_{uc-necessary}$, the uncertainty of the PV power, demand, and sudden interruption from the grid are considered to be obtained by the following equation:

$$E_{uc-necessary} = 2 * 1.33 * (|P_{total-error}(t)| + P_{grid}(t)) * 3^s / 3600, \quad (35)$$

where $P_{grid}(t)$ is the microgrid's exchanged power with the grid at time t and $P_{total-error}(t)$ is the sum of the forecasting error obtained by the following equation:

$$P_{total-error}(t) = (dP_{PV} - dP_{Load}) * noise. \quad (36)$$

The optimal size of the UC that is obtained by the PSO algorithm E_{uc-PSO} should be greater than Eq. (35).

At any time, half of the UC capacity should remain empty; therefore, the capacity used at all times is defined as:

$$E_{uc-mean} = \frac{E_{uc-PSO}}{2}. \quad (37)$$

At the time that the UCs are charged, they should be discharged so that they can be recharged for the next required charging time. Therefore, the excess amount of energy is conveyed to damp load, since half of its capacity should always remain empty.

When the UCs are discharged to avoid frequency drop, they will be recharged immediately for use at a later time.

UCs compensate errors by the following equation:

$$E_{uc}(t) = E_{uc-mean} + P_{total-error}(t) * 3^s / 3600. \quad (38)$$

3.6. Particle swarm optimization

The PSO formulation defines each particle as a potential solution to a problem in d -dimensional space with a memory of its previous best position and the best position among all of the particles, in addition to a velocity component. The particle dynamics in one dimension are given by:

$$v_{t+1} = w * v_t + c_1 * (p^{(l)} - x_t) + c_2 * (p^{(g)} - x_t), \quad (39)$$

$$x_{t+1} = x_t + v_{t+1}, \quad (40)$$

where v_t is the particle velocity at the t th iteration, x_t is the particle position at the t th iteration, $p^{(l)}$ is the personal best position or the particle's best position thus far, $p^{(g)}$ is the best global position or the best solution among all of the particles, w is the inertia factor, and c_1 and c_2 are the control coefficients. Particles draw their strength from their cooperative nature and are most effective when the cognitive (c_1) and social (c_2) coexist in a good balance, i.e. $c_1 \approx c_2$. If $c_1 \gg c_2$, each particle is very attracted to its own personal best position, resulting in excessive wandering.

On the other hand, if $c_2 \gg c_1$, the particles are more strongly attracted to the global best position, causing the particles to rush prematurely toward optima. For unimodal problems with a smooth search space, a larger social component will be efficient, whereas rough multimodal search spaces may find a larger cognitive component more advantageous.

Compared with other methods, PSO has the following advantages:

1. The algorithm is simple; there are not many parameters to be adjusted.
2. The algorithm is powerful; PSO is much faster for the above benchmark functions.

4. Simulation results

In this article, the optimum combination of the considered microgrid that is shown in Figure 1 is calculated. This system is optimized using the PSO algorithm. The software uses MATLAB programming. The lifetime of the project is 20 years.

The costs of the sold energy to the grid, the purchased energy from the grid, and the penalty for the interruption of the interruptible and uninterruptible loads are shown in Table 1.

Table 1. Costs of the sold energy to the grid, purchased energy from the grid, and the penalty for the interruption, interruptible, and uninterruptible loads.

Cost of the sold energy (\$/kWh)	Cost of the purchased energy (\$/kWh)	Penalty uninterruptible loads (\$/kWh)	Penalty interruptible loads (\$/kWh)
0.12	0.1	5.6	0.56

The system data consist of the annual solar radiation, which belongs to a region in northwestern Iran. The load curve, which is actually an IEEE standard curve with a 500 kW peak, is shown in Figure 2 [38].

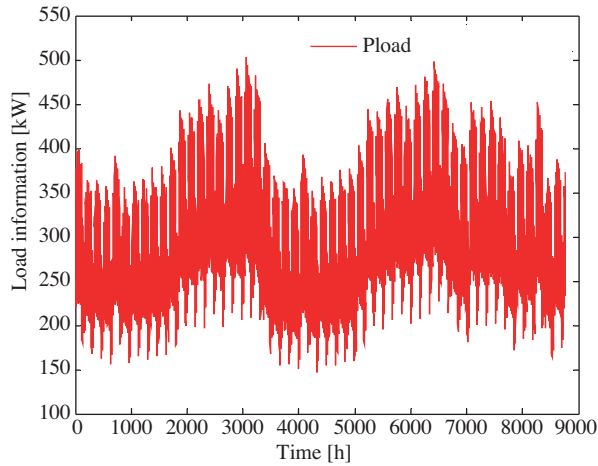


Figure 2. Load profile.

The power of the PV array could be derived by Eq. (34) and from the solar radiation data.

The optimal size of the PV array, battery pack and FC, interruptible and uninterruptible loads, and exchanged power with the grid are shown in Tables 2 and 3.

Table 2. Optimal size of each component.

PV array	Battery pack	Fuel cell	Trans (kW)	Ultracapacitors (kWh)	Total cost (\$)
764	2	332	100	1.15038	7,444,000

Table 3. Optimal size of the exchanged power and interruptible and uninterruptible loads.

Interruptible loads (kWh)	Uninterruptible loads (kWh)	Purchased power (kWh)	Sold power (kWh)
9.0482×10^3	718.5439	96.0175×10^3	126.1933

Figures 3 and 4 show the energy of the battery storages and the output power of the FCs, respectively.

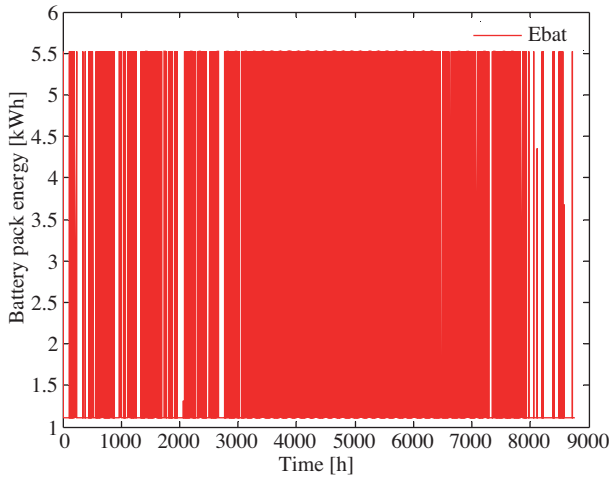


Figure 3. Energy variations of the battery packs.

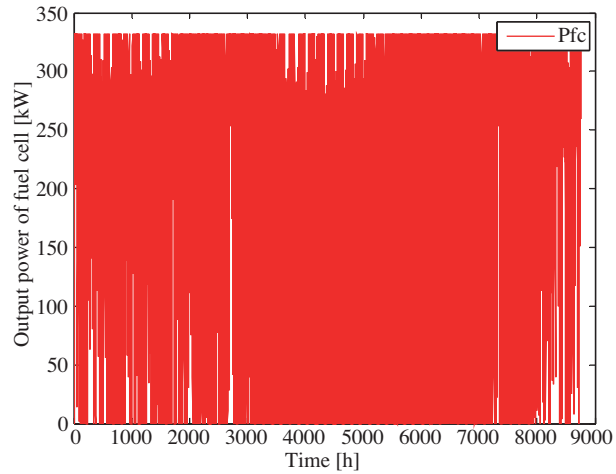


Figure 4. Output power of the fuel cells.

Figures 5 and 6 show that the interruptible and uninterruptible loads in each hour are not supported.

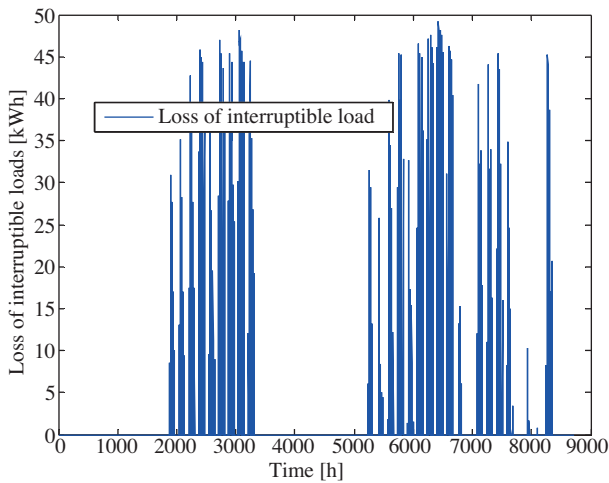


Figure 5. Loss of interruptible loads in each hour.

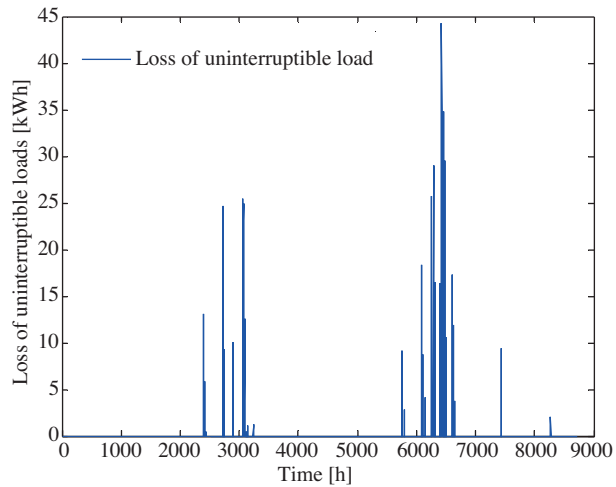


Figure 6. Loss of uninterruptible loads in each hour.

Figure 7 shows the purchased energy from the grid and Figure 8 shows the sold energy to the grid for each hour.

Figure 9 shows the total uncertainties of the power generation of the PV arrays and demand.

Figure 10 shows the energy variations of the UCs.

The total cost of the microgrid considering the penalties, purchased energy from the grid, and the sold energy to the grid is equal to \$7,507,400.

At the time between 6200 and 6700, the FCs inject power into the microgrid. At these times, the purchased power from the grid is equal to the maximum level. Therefore, the microgrid sheds the interruptible and uninterruptible loads.

At times 3000 and 6500, the load peak occurred. At these times, the produced power in the microgrid plus the purchased energy from the grid cannot satisfy the demand. Figures 4 and 5 show that interruptible and uninterruptible loads at these hours are interrupted. Figure 2 shows that the demand of the microgrid at

the hours between 4000 and 5000 is less than at other times; therefore, the produced power of the microgrid and the purchased energy from the grid can meet the demand and loads will not be interrupted. The amounts of some notions of the reliability are shown in Table 4. Table 4 shows that the ELF is in the acceptable confine.

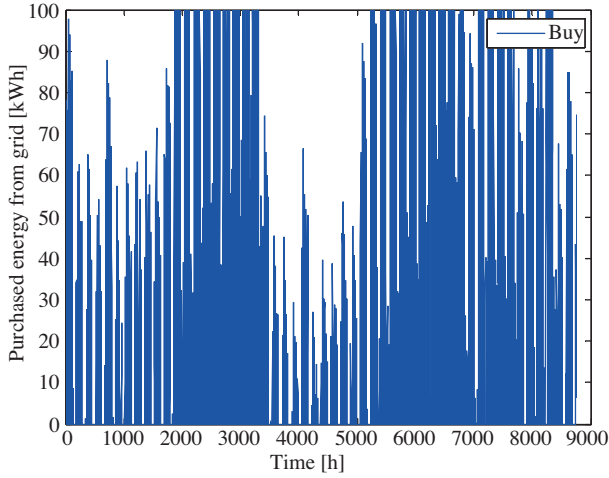


Figure 7. Purchased energy from grid.

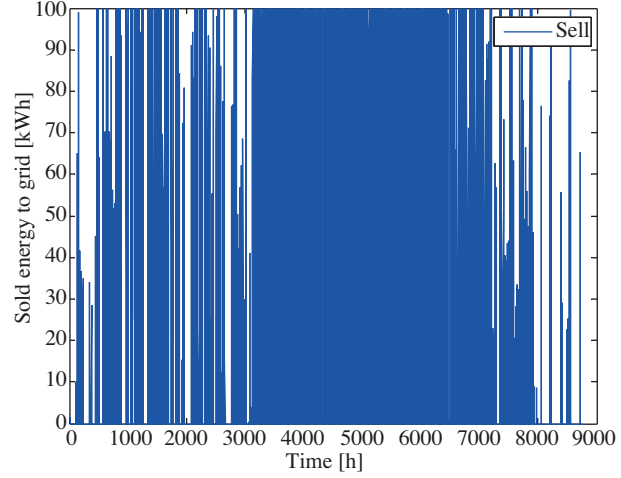


Figure 8. Sold energy to grid.

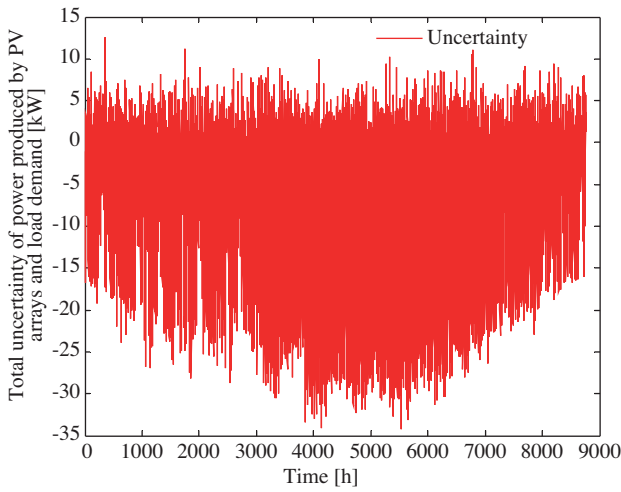


Figure 9. Total uncertainty of power generation of the PV arrays and load demand.

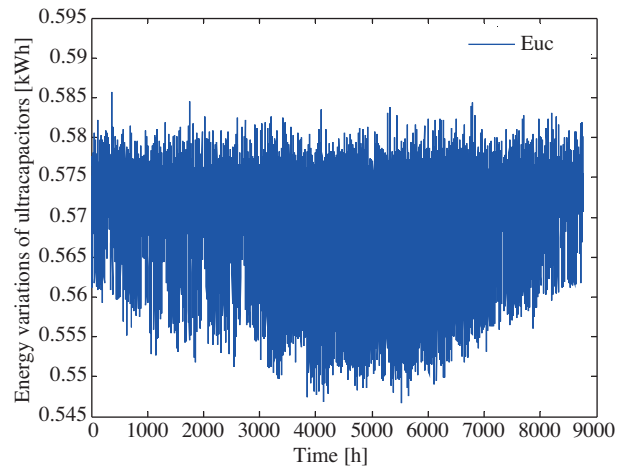


Figure 10. Energy variations of the UCs.

Table 4. Amount of some notions of reliability.

LOLE (h/year)	LPSP	LOEE (MWh/year)	ELF
60	293.4361×10^{-6}	0.71854	175.77×10^{-6}

Figure 11 shows the system costs in terms of the iterations.

In this study, we also use a GA for solving this minimization problem. The results of this algorithm are similar to those of the PSO algorithm.

5. Effect of amount of interruptible loads on cost of the microgrid

In this section, the effect of the amount of the interruptible loads on the total cost of the microgrid is evaluated. First, we consider that all of the loads are uninterruptible. Next, the interruptible loads are considered and increased from 10% to 40% of the load.

The total cost of the microgrid at several levels of interruptible loads is shown in Figure 12.

Figure 12 shows that increasing the amount of interruptible loads in the microgrid causes the total cost of the microgrid to decrease.

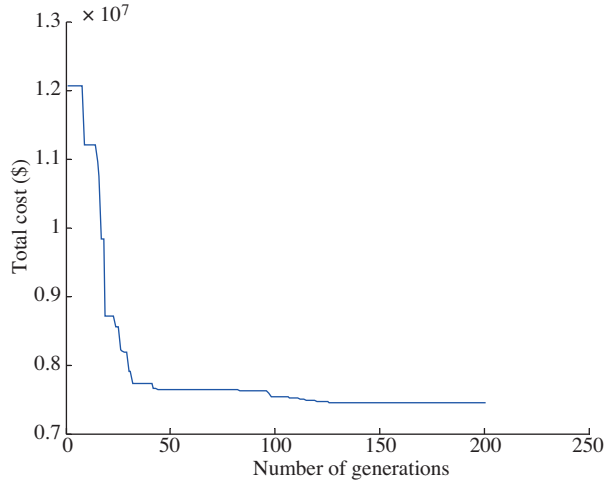


Figure 11. The cost of the microgrid in terms of the iterations.

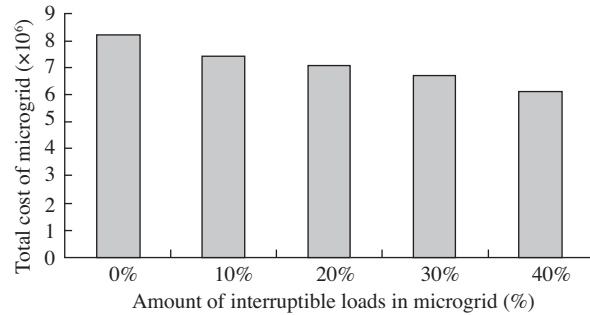


Figure 12. Total cost of microgrid in several levels of interruptible loads.

6. Conclusion

In this paper, the optimal size of a microgrid was considered. The system consists of PV/FC, battery packs, and UCs. The interruptible and uninterruptible loads for the microgrid were considered and the microgrid can exchange power with the grid.

The optimal size for all of the microgrid components was considered. In addition, the optimal size of the UCs was obtained in order to compensate for the power fluctuations due to the uncertainty of output power of the PV arrays and required loads in the microgrid, as well as the sudden interruption from the grid. The main problem of renewable energy sources is that they are dependent on environmental conditions. Hence, they could not cover the demand perfectly. Adding a storage component solves this problem significantly. In this study, a battery pack was used to cover the demand desirably.

The microgrid that was used in this study has high reliability, since FCs were utilized as a backup for the PV arrays, especially in islanded operation.

The simulation results showed that considering interruptible loads for the microgrid results in cost reduction for the microgrid. To ensure the system's reliability, the FOR, reliability parameters, and the uncertainty of the PV power and load demand were considered.

References

- [1] R. Lasseter, A. Akhil, C. Marnay, J. Stephens, J. Dagle, R. Guttromson, A. Meliopoulos, R. Yinger, J. Eto, White paper on Integration of Consortium Energy Resources. The CERTS MicroGrid Concept, CERTS, Rep. LBNL-50829, 2002.
- [2] MICROGRIDS: Large Scale Integration of Micro-Generation to Low Voltage Grids, EU Contact ENK5-CT-2002-00610, Technical Annex, 2002.
- [3] W. Deng, W. Pei, Z. Qi, “Impact and improvement of distributed generation on voltage quality in micro-grid”, 3rd International Conference on Electric Utility Deregulation and Restructuring and Power Technologies, pp. 1737–1741, 2008.
- [4] R.H. Lasseter, “Microgrids”, IEEE Power Engineering Society Winter Meeting, Vol. 1, pp. 305–308, 2002.
- [5] C. Marnay, G. Venkataramanan, “Microgrids in the evolving electricity generation and delivery infrastructure”, IEEE Power Engineering Society General Meeting, pp. 18–22, 2006.
- [6] O. Özgönel, D.W.P. Thomas, “Short-term wind speed estimation based on weather data”, Turkish Journal of Electrical Engineering & Computer Sciences, Vol. 20, pp. 335–346, 2012.
- [7] M. Uzunoglu, O.C. Onar, M.S. Alam, “Modeling, control and simulation of a PV/FC/UC based hybrid power generation system for stand-alone applications”, Renewable Energy, Vol. 34, pp. 509–520, 2009.
- [8] D. Menniti, A. Pinnarelli, N. Sorrentino, “A method to improve microgrid reliability by optimal sizing PV/WIND plants and storage systems”, 20th International Conference on Electricity Distribution, 2009.
- [9] Y.G. Rebours, D.S. Kirschen, M. Trotignon, S. Rossignol, “A survey of frequency and voltage control ancillary services—Part I: technical features”, IEEE Transactions on Power Systems, Vol. 22, pp. 350–357, 2007.
- [10] H.L. Willis, W.G. Scott, Distributed Power Generation: Planning and Evaluation, New York, Marcel Dekker, 2000.
- [11] B.S. Borowy, Z.M. Salameh, “Methodology for optimally sizing the combination of a battery bank and PV array in a wind/PV hybrid system”, IEEE Transactions on Energy Conversion, Vol. 11, pp. 367–375, 1996.
- [12] S.S. Dhrab, K. Sopian, “Electricity generation of hybrid PV/wind systems in Iraq”, Renewable Energy, Vol. 35, pp. 1303–1307, 2010.
- [13] M.A. Habib, S.A.M. Said, M.A. El-Hadidy, A.I. Zaharna, “Optimization procedure of hybrid photovoltaic wind energy system energy”, Energy, Vol. 24, pp. 919–929, 1999.
- [14] J.K. Kaldellis, “Parametric investigation concerning dimensions of a stand-alone wind-power system”, Applied Energy, Vol. 77, pp. 35–50, 2004.
- [15] B. Ai, H. Yang, H. She, X. Liao, “Computer-aided design of PV/wind hybrid system”, Renewable Energy, Vol. 28, pp. 1491–1512, 2003.
- [16] M.A. Elhadidy, S.M. Shaahid, “Optimal sizing of battery storage for hybrid (wind+diesel) power systems”, Renewable Energy, Vol. 18, pp. 77–86, 1999.
- [17] A.M. Al-Ashwal, I.S. Moghram, “Proportion assessment of combined PV-wind generating systems”, Renewable Energy, Vol. 10, pp. 43–51, 1997.
- [18] Ö. Atlam, “A small scale education experiment kit with wind generator-PEM electrolyser system and modeling”, Turkish Journal of Electrical Engineering & Computer Sciences, Vol. 18, pp. 583–595, 2010.
- [19] B. Dursun, C. Gökçöl, “Economic analysis of a wind-battery hybrid system: an application for a house in Gebze, Turkey, with moderate wind energy potential”, Turkish Journal of Electrical Engineering & Computer Sciences, Vol. 20, pp. 319–333, 2012.
- [20] A.H. Shahirinia, S.M.M. Tafreshi, A. Hajizadeh Gastaj, A.R. Moghaddamjoo, “Optimal sizing of hybrid power system using genetic algorithm”, International Conference on Future Power Systems, 2005.
- [21] S. Ghaemi, S.M. Moghaddas-Tafreshi, Optimal Sizing of Grid-Connected Hybrid Power System in Qeshm Island in Persian Gulf of Iran, Vienna, IEWT, 2007.

- [22] S.C. Gupta, Y. Kumar, G. Agnihotri, "Optimal sizing of solar-wind hybrid system", IET-UK International Conference on Information and Communication Technology in Electrical Sciences, pp. 282–287, 2007.
- [23] G. La Terra, G. Salvina, T.G. Marco, "Optimal sizing procedure for hybrid solar wind power systems by fuzzy logic", IEEE Mediterranean Electrotechnical Conference, pp. 865–868, 2006.
- [24] M. Uzunoglu, O.C. Onar, M.S. Alam, "Modeling, control and simulation of a PV/FC/UC based hybrid power generation system for stand-alone applications", *Renewable Energy*, Vol. 34, pp. 509–520, 2009.
- [25] D. Xu, L. Kang, B. Cao, "Optimal sizing of standalone hybrid wind/PV power systems using genetic algorithms", Proceedings of the IEEE Canadian Conference on Electrical and Computer Engineering, pp. 1705–1708, 2005.
- [26] A.A. Kulaksız, R. Akkaya, "Training data optimization for ANNs using genetic algorithms to enhance MPPT efficiency of a stand-alone PV system", *Turkish Journal of Electrical Engineering & Computer Sciences*, Vol. 20, pp. 241–254, 2012.
- [27] M.J. Khan, M.T. Iqbal, "Pre-feasibility study of stand-alone hybrid energy systems for applications in Newfoundland", *Renewable Energy*, Vol. 30, pp. 835–854, 2005.
- [28] M. Brown, T.R. Casten, *Guide to Decentralized Energy Technologies*, Edinburgh, World Alliance for Decentralized Energy, 2003.
- [29] H. Liu, C. Mao, "Electronic power transformer with supercapacitors storage energy system", *Electric Power Systems Research*, Vol. 79, pp. 1200–1208, 2009.
- [30] C.M. Kyung, S. Yoo, *Energy-Aware System Design: Algorithms and Architectures*, New York, Springer, 2011.
- [31] H. Hassanzadeh-Fard, S.M. Moghaddas-Tafreshi, S.M. Hakimi, "Optimal sizing of an islanded micro-grid for an area in north-west Iran using particle swarm optimization based on reliability concept", *World Renewable Energy Congress*, Vol. 11, pp. 2969–2976, 2011.
- [32] S.M. Hakimi, S.M. Moghaddas-Tafreshi, "Optimal sizing of a stand-alone hybrid power system via particle swarm optimization for Kahnouj area in south-east of Iran", *Renewable Energy*, Vol. 34, pp. 1855–1862, 2009.
- [33] R.S. Garcia, D. Weisser, "A wind-diesel system with hydrogen storage: joint optimization of design and dispatch", *Renewable Energy*, Vol. 31, pp. 2296–2320, 2006.
- [34] A. Kashefi Kaviani, G.H. Riahy, S.H.M. Kouhsari, "Optimal design of a reliable hydrogen-based stand-alone wind/PV generating system, considering component outages", *Renewable Energy*, Vol. 34, pp. 2380–2390, 2009.
- [35] Bagen, R. Billinton, "Evaluation of different operating strategies in small stand-alone power systems", *IEEE Transactions on Energy Conversion*, Vol. 20, pp. 654–660, 2005.
- [36] R. Karki, R. Billinton, "Reliability/cost implications of PV and wind energy utilization in small isolated power systems", *IEEE Transactions on Energy Conversion*, Vol. 16, pp. 368–373, 2001.
- [37] X. Li, Y.J. Song, S.B. Han, "Frequency control in micro-grid power system combined with electrolyzer system and fuzzy PI controller", *Journal of Power Sources*, Vol. 180, pp. 468–475, 2008.
- [38] Reliability Test System Task Force of the IEEE Subcommittee on the Application of Probability Methods, "IEEE reliability test system", *IEEE Transactions on Power Apparatus and Systems*, Vol. PAS-98, pp. 2047–2054, 1979.